

Spectroscopic Properties of Er³⁺ Doped Zinc Lithium Arsenic Strontium Vanadium Bismuth Borate Glasses

S.L.Meena

Ceramic Laboratory, Department of physics, Jai Narain Vyas University, Jodhpur 342001(Raj.)Ind

Abstract

Zinc lithium arsenic strontium vanadium bismuth borate glasses containing Er³⁺ in (35- x): Bi₂O₃:10ZnO:10Li₂O:10As₂O:10SrO₂:10V₂O₅:15B₂O₃:xEr₂O₃ (where x=1, 1.5,2 mol %) have been prepared by melt-quenching method. The amorphous nature of the glasses was confirmed by x-ray diffraction studies. Optical absorption and fluorescence spectra were recorded at room temperature for all glass samples. Judd-Ofelt intensity parameters Ω_{λ} ($\lambda=2, 4, 6$) are evaluated from the intensities of various absorption bands of optical absorption spectra. Using these intensity parameters various radiative properties like spontaneous emission probability, branching ratio, radiative life time and stimulated emission cross-section of various emission lines have been evaluated.

Keywords: ZLASVBB Glasses, Optical Properties, Judd-Ofelt Theory, Rare earth ions.

Date of Submission: 27-11-2020

Date of Acceptance: 11-12-2020

I. Introduction

Glasses doped with various rare-earth ions are important materials for fluorescent display devices, optical detectors, optical fibers and optical amplifiers [1-3]. Among the other heavy metal oxide glasses, bismuth borate glasses have wide range of applications in the field of glass ceramics, layers for optical and electronic devices, thermal and mechanical sensors, reflecting windows [4,5], Glasses containing heavy metal oxides exhibits good non-linear optical properties and good chemical durability [6,7]. The past literature shows that the rare earth ions find more important application in the preparation of the laser materials [8, 9].

Among various glasses, borate glasses are excellent host matrices because boric oxide (B₂O₃) acts as a good glass former and flux material [10]. ZnO is a wide band gap semiconductor and has received increasing research interest. It is an important multifunction material due to its specific chemical, surface and micro structural properties. It is used in various applications such as gas sensor, varistors, catalysts etc. [11]. Er³⁺ ion is the most studied among the rare earth ions and the up conversion process of this ion in various kinds of host materials has been investigated [12-16].

The present work reports on the preparation and characterization of rare earth doped heavy metal oxide (HMO) glass systems for lasing materials. I have studied on the absorption, excitation and emission properties of Er³⁺ doped zinc lithium arsenic strontium vanadium bismuth borate glasses. The intensities of the transitions for the rare earth ions have been estimated successfully using the Judd-Ofelt theory. The laser parameters such as radiative probabilities (A), branching ratio (β), radiative life time (τ_R) and stimulated emission cross section (σ_p) are evaluated using J.O. intensity parameters (Ω_{λ} , $\lambda=2, 4$ and 6).

II. Experimental Techniques

Preparation of glasses

The following Er³⁺ doped zinc lithium arsenic strontium vanadium bismuth borate glass samples (35-x) Bi₂O₃:10ZnO:10Li₂O:10As₂O:10SrO₂:10V₂O₅:15 B₂O₃: xEr₂O₃. (where x=1, 1.5,2) have been prepared by melt-quenching method. Analytical reagent grade chemical used in the present study consist of Bi₂O₃, ZnO, Li₂O, As₂O, SrO₂, V₂O₅ and B₂O₃ and Er₂O₃. All weighed chemicals were powdered by using an Agate pestle mortar and mixed thoroughly before each batch (10g) was melted in alumina crucibles in silicon carbide based electrical furnace.

Silicon Carbide Muffle furnace was heated to working temperature of 1050⁰C, for preparation of zinc lithium arsenic strontium vanadium bismuth borate glasses, for two hours to ensure the melt to be free from gases. The melt was stirred several times to ensure homogeneity. For quenching, the melt was quickly poured on the steel plate & was immediately inserted in the muffle furnace for annealing. The steel plate was preheated to 100⁰C. While pouring; the temperature of crucible was also maintained to prevent crystallization. And annealed at temperature of 355⁰C for 2h to remove thermal strains and stresses. Every time fine powder of cerium oxide was used for polishing the samples. The glass samples so prepared were of good optical quality

and were transparent. The chemical compositions of the glasses with the name of samples are summarized in Table 1

Table 1 Chemical composition of the glasses

Sample	Glass composition (mol %)
ZLASVBB (UD)	35 Bi ₂ O ₃ :10ZnO:10Li ₂ O:10As ₂ O:10SrO ₂ :10V ₂ O ₅ :15B ₂ O ₃
ZLASVBB (ER1)	34 Bi ₂ O ₃ :10ZnO:10Li ₂ O:10As ₂ O:10SrO ₂ :10V ₂ O ₅ :15B ₂ O ₃ :1 Er ₂ O ₃
ZLASVBB (ER 1.5)	33.5 Bi ₂ O ₃ :10ZnO:10Li ₂ O:10As ₂ O:10SrO ₂ :10V ₂ O ₅ :15B ₂ O ₃ : 1.5 Er ₂ O ₃
ZLASVBB (ER 2)	33 Bi ₂ O ₃ :10ZnO:10Li ₂ O:10As ₂ O:10SrO ₂ :10V ₂ O ₅ :15B ₂ O ₃ : 2 Er ₂ O ₃

ZLASVBB (UD)—Represents undoped Zinc Lithium Arsenic Strontium Vanadium Bismuth Borate glass specimens.

ZLASVBB (ER) -Represents Er³⁺ doped Zinc Lithium Arsenic Strontium Vanadium Bismuth Borate glass specimens.

III. Theory

3.1 Oscillator Strength

The intensity of spectral lines are expressed in terms of oscillator strengths using the relation [17].

$$f_{\text{expt.}} = 4.318 \times 10^{-9} \int \epsilon(\nu) d\nu \quad (1)$$

where, $\epsilon(\nu)$ is molar absorption coefficient at a given energy ν (cm⁻¹), to be evaluated from Beer–Lambert law.

Under Gaussian Approximation, using Beer–Lambert law, the observed oscillator strengths of the absorption bands have been experimentally calculated, using the modified relation [18].

$$P_m = 4.6 \times 10^{-9} \times \frac{1}{cl} \log \frac{I_0}{I} \times \Delta\nu_{1/2} \quad (2)$$

where c is the molar concentration of the absorbing ion per unit volume, l is the optical path length, $\log I_0/I$ is absorptivity or optical density and $\Delta\nu_{1/2}$ is half band width.

3.2. Judd-Ofelt Intensity Parameters

According to Judd [19] and Ofelt [20] theory, independently derived expression for the oscillator strength of the induced forced electric dipole transitions between an initial J manifold $|4f^N(S, L) J\rangle$ level and the terminal J' manifold $|4f^N(S', L') J'\rangle$ is given by:

$$\frac{8\pi^2 mc \bar{\nu}}{3h(2J+1)n} \frac{1}{n} \left[\frac{(n^2+2)^2}{9} \right] \times S(J, J') \quad (3)$$

where, the line strength $S(J, J')$ is

given by the equation

$$S(J, J') = e^2 \sum_{\lambda} \Omega_{\lambda} \langle 4f^N(S, L) J \| U^{(\lambda)} \| 4f^N(S', L') J' \rangle^2 \quad (4)$$

$\lambda = 2, 4, 6$

In the above equation m is the mass of an electron, c is the velocity of light, ν is the wave number of the transition, h is Planck's constant, n is the refractive index, J and J' are the total angular momentum of the initial and final level respectively, Ω_{λ} ($\lambda = 2, 4$ and 6) are known as Judd-Ofelt intensity.

3.3. Radiative Properties

The Ω_{λ} parameters obtained using the absorption spectral results have been used to predict radiative properties such as spontaneous emission probability (A) and radiative life time (τ_R), and laser parameters like fluorescence branching ratio (β_R) and stimulated emission cross section (σ_p).

The spontaneous emission probability from initial manifold $|4f^N(S', L') J'\rangle$ to a final manifold $|4f^N(S, L) J\rangle$ is given by:

$$A [(S', L') J'; (S, L) J] = \frac{64 \pi^2 \nu^3}{3h(2J'+1)} \left[\frac{n(n^2+2)^2}{9} \right] \times S(J', \bar{J}) \quad (5)$$

Where, $S(J', J) = e^2 [\Omega_2 \| U^{(2)} \|^2 + \Omega_4 \| U^{(4)} \|^2 + \Omega_6 \| U^{(6)} \|^2]$

The fluorescence branching ratio for the transitions originating from a specific initial manifold $|4f^N(S', L') J'\rangle$ to a final many fold $|4f^N(S, L) J\rangle$ is given by

$$\beta [(S', L') J'; (S, L) J] = \frac{A[(S', L) J]}{A[(S', L') J'] + A[(S, L) J]} \quad (6)$$

The radiative life time is given by
 $\tau_{rad} = \sum_{S, L, J} A[(S', L') J'; (S, L) J] = A_{Total}^{-1} \quad (7)$

where, the sum is over all possible terminal manifolds. The stimulated emission cross -section for a transition from an initial manifold $|4f^N (S', L') J\rangle$ to a final manifold $|4f^N (S, L) J\rangle$ is expressed as

$$\sigma_p(\lambda_p) = \left[\frac{\lambda_p^4}{8\pi c n^2 \Delta\lambda_{eff}} \right] \times A[(S', L') J'; (\bar{S}, \bar{L}) \bar{J}] \quad (8)$$

where, λ_p the peak fluorescence wavelength of the emission band and $\Delta\lambda_{eff}$ is the effective fluorescence line width.

IV. Result and Discussion

4.1. XRD Measurement

Figure 1 presents the XRD pattern of the samples containing show no sharp Bragg's peak, but only a broad diffuse hump around low angle region. This is the clear indication of amorphous nature with in the resolution limit of XRD instrument.

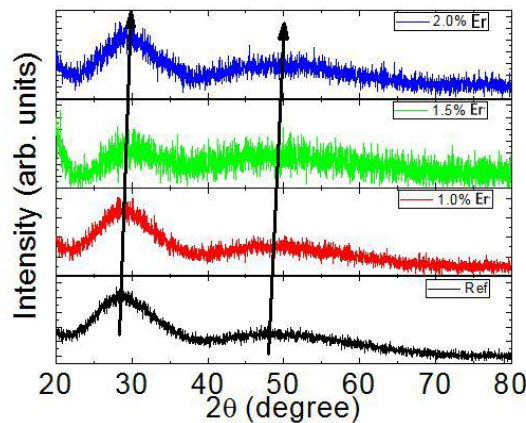


Fig.1:X-ray diffraction pattern of ZLASVBB (ER) glasses.

4.2. Absorption spectra

The absorption spectra of ZLASVBB (ER) glasses, consists of absorption bands corresponding to the absorptions from the ground state $^4I_{15/2}$ of Er^{3+} ions. Ten absorption bands have been observed from the ground state $^4I_{15/2}$ to excited states $^4I_{11/2}$, $^4I_{9/2}$, $^4F_{9/2}$, $^4S_{3/2}$, $^2H_{11/2}$, $^4F_{7/2}$, $^4F_{5/2}$, $^4F_{3/2}$, $^2H_{9/2}$ and $^4G_{11/2}$ for Er^{3+} doped ZLASVBB (ER)glasses.

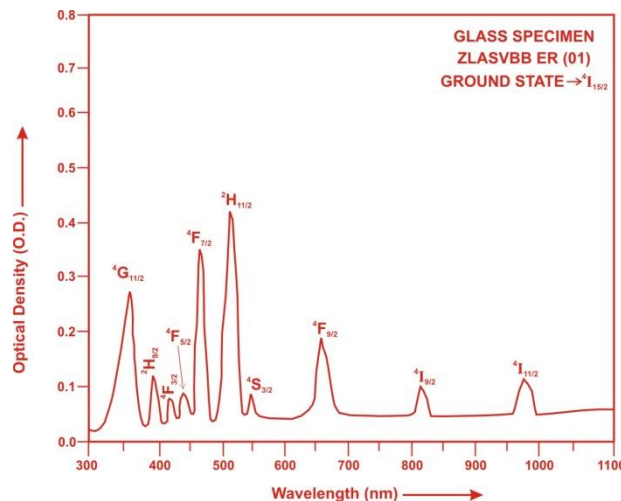


Fig.2: Absorption spectra of ZLASVBB (ER) glasses.

The experimental and calculated oscillator strengths for Er³⁺ ions in zinc lithium arsenic strontium vanadiumbismuth borate glasses are given in **Table 2**

Table 2. Measured and calculated oscillator strength ($P^m \times 10^{+6}$) of Er³⁺ ions in ZLASVBB glasses.

Energy level ⁴ I _{15/2}	Glass ZLASVBB (ER01)		Glass ZLASVBB (ER1.5)		Glass ZLASVBB (ER02)	
	P _{exp.}	P _{cal.}	P _{exp.}	P _{cal.}	P _{exp.}	P _{cal.}
⁴ I _{11/2}	0.88	0.74	0.82	0.74	0.76	0.74
⁴ I _{9/2}	0.45	0.16	0.38	0.15	0.32	0.15
⁴ F _{9/2}	2.46	1.58	2.41	1.57	2.35	1.57
⁴ S _{3/2}	0.38	0.67	0.32	0.67	0.27	0.67
² H _{11/2}	6.46	2.60	6.42	2.61	6.37	2.63
⁴ F _{7/2}	5.38	2.32	5.32	2.32	5.27	2.32
⁴ F _{5/2}	0.62	0.85	0.58	0.85	0.52	0.85
⁴ F _{3/2}	0.38	0.52	0.32	0.52	0.27	0.52
² H _{9/2}	1.72	0.99	1.68	0.99	1.62	0.99
⁴ G _{11/2}	4.68	6.28	4.62	6.30	4.57	6.33
R.m.s.deviation	1.6862		1.6676		1.6478	

The various energy interaction parameters like Slater-Condon parameters F_k ($k=2, 4, 6$), Lande' parameter (ξ_{4f}) and Racah parameters E^k ($k=1, 2, 3$) have been computed using partial regression method and formula described elsewhere [21]. The ratio of Racah parameters E^1/E^3 and E^2/E^3 are about 10.349 and 0.0487 respectively. Which are almost equal to the hydrogenic ratio [22]. This implies that Er³⁺ ions at different doping concentrations are subjected. Computed values of Slater-Condon, Lande', Racah, nephelauxetic ratio and bonding parameter for Er³⁺ doped ZLASVBB glass specimens are given in **Table 3**.

Table 3. Computed values of Slater-Condon, Lande', Racah, nephelauxetic ratio and bonding parameter for Er³⁺ doped ZLASVBB glass specimens.

Parameter	Free ion	ZLASVBB(ER01)	ZLASVBB(ER1.5)	ZLASVBB(ER02)
$F_2(\text{cm}^{-1})$	441.680	433.919	433.898	433.877
$F_4(\text{cm}^{-1})$	68.327	67.042	67.0452	67.0596
$F_6(\text{cm}^{-1})$	7.490	7.0403	7.0396	7.03994
$\xi_{4f}(\text{cm}^{-1})$	2369.400	2414.810	2414.826	2414.752
$E^1(\text{cm}^{-1})$	6855.300	6661.750	6661.507	6661.791
$E^2(\text{cm}^{-1})$	32.126	31.341	31.3378	31.3308
$E^3(\text{cm}^{-1})$	645.570	643.726	643.720	643.703
F_4/F_2	0.15470	0.1545	0.15452	0.154559
F_6/F_2	0.01696	0.01622	0.0162240	0.016226
E^1/E^3	10.61899	10.349	10.348	10.349
E^2/E^3	0.049764	0.048688	0.0486823	0.048673
β'		0.98243	0.98238	0.98233
$b^{1/2}$		0.093728	0.093862	0.093995

Judd-Ofelt intensity parameters Ω_λ ($\lambda = 2, 4$ and 6) were calculated by using the fitting approximation of the experimental oscillator strengths to the calculated oscillator strengths with respect to their electric dipole contributions. In the present case the three Ω_λ parameters follow the trend $\Omega_4 < \Omega_2 < \Omega_6$.

The values of Judd-Ofelt intensity parameters are given in **Table 4**.

Table 4. Judd-Ofelt intensity parameters for Er³⁺ doped ZLASVBB glass specimens.

Glass Specimen	$\Omega_2(\text{pm}^2)$	$\Omega_4(\text{pm}^2)$	$\Omega_6(\text{pm}^2)$	Ω_4/Ω_6
ZLASVBB(ER01)	0.7729	0.2780	0.8744	0.318
ZLASVBB(ER1.5)	0.7822	0.2699	0.8766	0.308
ZLASVBB(ER02)	0.7925	0.2611	0.8795	0.297

4.3 Excitation Spectrum

The Excitation spectra of Er³⁺ doped ZLASVBB glass specimens have been presented in Figure 3 in terms of Excitation Intensity versus wavelength. The excitation spectrum was recorded in the spectral region 300–600 nm fluorescence at 550nm having different excitation band centered at 350, 365, 380, 425, 450, 470 and 515 nm are attributed to the ²K_{15/2}, ⁴G_{9/2}, ⁴G_{11/2}, ²G_{9/2}, ⁴F_{3/2}, ⁴F_{5/2} and ²H_{11/2} transitions, respectively. The highest absorption level is ⁴G_{11/2} and is at 381nm. So this is to be chosen for excitation wavelength.

V. Conclusion

In the present study, the glass samples of composition (35-x) Bi₂O₃:10ZnO:10Li₂O:10As₂O:10SrO₂:10V₂O₅:15B₂O₃:xEr₂O₃ (where x=1, 1.5, 2 mol %) have been prepared by melt-quenching method. The value of stimulated emission cross-section (σ_p) is found to be maximum for the transition ($^4F_{7/2} \rightarrow ^4I_{15/2}$) for glass ZLASVBB (ER 01), suggesting that glass ZLASVBB (ER 01) is better compared to the other two glass systems ZLASVBB(ER1.5) and ZLASVBB (ER02). The radiative transition probability and the branching ratio are highest for ($^4F_{7/2} \rightarrow ^4I_{15/2}$) transition and hence it is useful for laser action.

References:

- [1]. Vijaya, N., and Jayasankar, C.K. (2013). Structural and spectroscopic properties of Eu³⁺ - doped zinc fluorophosphate glasses, *J. Mol. Struct.* 1036, 42–50.
- [2]. Martin, R.A. and Knight, J.C. (2006). Silica-clad neodymium-doped lanthanum phosphate fibers and fiber lasers, *IEEE Photon Technol. Lett.* 18(4), 574-576.
- [3]. Ramteke, D.D., Annapurna, K., Deshpande, V.K. and Gedam, R.S. (2014). Effect of Nd³⁺ on spectroscopic properties of lithium borate glasses, *Journal of Rare Earth*, 32, 1148-1153.
- [4]. Kothandan, D. and Kumar, R. J. (2015). Optical properties of rare earth doped borate glasses, *International Journal of ChemTech Research* 8(6), 310-314.
- [5]. Pawar, P. P., Munishwar, S.R. and Gedam, R.S. (2016). Physical and optical properties of Dy³⁺/Pr³⁺ co-doped lithium borate glasses for W-LED, *Journal of Alloys and Compounds*, 660, 347-355.
- [6]. Prabhu, N. S., MI Sayyed V. H., Agar, O. and Kamath, S. D. (2019). Investigations on structural and radiation shielding properties of Er³⁺ doped zinc bismuth borate glasses, *Materials chemistry and physics*, 230, 267-276.
- [7]. Patwari, R. and Eraiah, B. (2019). Optical and Plasmonic properties of Er³⁺ and silver co-doped borate nano-composite glasses, *Materials Research Express* 6(11), 116218.
- [8]. Shanmuga, S. S., Marimuthu, K., Sivraman, M. and Babu, S. S. (2010). Composition dependent structural and optical properties of Sm³⁺-doped sodium borate and sodium fluoroborate glasses, *Journal of Luminescence*, 130, 1313–1319.
- [9]. Lin, H., E. V. B. and Wang, X. J. (2005). Intense visible fluorescence and energy transfer in Dy³⁺, Tb³⁺, Sm³⁺, and Eu³⁺ doped rare earth borate glasses, *Journal of Alloys and Compounds*, 390, 197-201.
- [10]. Jianber, QIU, Qing, JIAQ, Dacheng, ZHOU, Zhengwen YANG Zhengwen (2016). Recent progress on upconversion enhancement in rare earth doped transparent glass ceramics, *Journal of Rare Earths* 34(4), 341-367.
- [11]. Wojciech, A., Piasarski, Tomasz Goryezka, Joanna, P. and Romanowski, W. R. Romanowski (2007). Er doped lead Borate Glasses and Transparent Glass Ceramics for near infrared luminescence and up-conversion applications, "The Journal of Physical Chemistry.
- [12]. Guo, J., Liu, X., Duan, G., Yang, Y., Zhao, G., Huang, F., Bai, G. and Zhang, J. (2019). Optimization by energy transfer process of 2.7 μ m emission in highly Er³⁺-doped tungsten-tellurite glasses. *Infrared Phys. Technol.* 99, 49–54.
- [13]. Weng, F., Chen, D., Wang, Y., Yu, Y., Huang, P., Lin, H. (2009). Energy transfer and up-conversion luminescence in Er³⁺/Yb³⁺ co-doped transparent glass ceramic containing YF₃ nano-crystals. *Ceram. Int.* 35, 2619–2623.
- [14]. Qiao, X., Fan, X., Wang, M. (2006). Luminescence behavior of Er³⁺ in glass ceramics containing BaF₂ nanocrystals. *Scr. Mater.* 55, 211–214.
- [15]. Nazrin, S.N., Halimah, M.K., Muhammad, F.D., Yip, J.S., Hasnimulyati, L., Faznny, M.F. and Zaitizila, I. (2018). The effect of erbium oxide in physical and structural properties of zinc tellurite glass system. *J. Non Cryst. Solids* 490, 35–43.
- [16]. Farouk, M., Samir, A., Metawe, F. and Elokr, M. (2013). Optical absorption and structural studies of bismuth borate glasses containing Er³⁺ ions. *J. Non-Cryst. Solids* 371–372, 14–21.
- [17]. Gorller-Walrand, C. and Binnemans, K. (1988) Spectral Intensities of f-f Transition. In: Gshneidner Jr., K.A. and Eyring, L., Eds., *Handbook on the Physics and Chemistry of Rare Earths*, Vol. 25, Chap. 167, North-Holland, Amsterdam, 101-264.
- [18]. Sharma, Y.K., Surana, S.S.L. and Singh, R.K. (2009) Spectroscopic Investigations and Luminescence Spectra of Sm³⁺ Doped Soda Lime Silicate Glasses. *Journal of Rare Earths*, 27, 773-780.
- [19]. Judd, B.R. (1962). Optical Absorption Intensities of Rare Earth Ions. *Physical Review*, 127, 750-761.
- [20]. Ofelt, G.S. (1962) Intensities of Crystal Spectra of Rare Earth Ions. *The Journal of Chemical Physics*, 37, 511.
- [21]. Sharma, Y.K. (1991). Spectral and Electrol Properties of Lanthanide Ions in Different Environment. PhD Thesis, University of Jodhpur, Jodhpur.
- [22]. Dieke, G.H. (1968). Spectra and Energy Levels of Rare Earth Ions in Crystals. InterScience, Johan Wiley and Sons, New York.

S.L.Meena. "Spectroscopic Properties of Er³⁺ Doped Zinc Lithium Arsenic Strontium Vanadium Bismuth Borate Glasses." *IOSR Journal of Applied Physics (IOSR-JAP)*, 12(6), 2020, pp. 05-10.